recycling

MDPI

Article

Mechanical Decrosslinking and Reprocessing of Crosslinked Rotomolded Polypropylene Using Cryogenic-Assisted Shear Pulverization and Compression Molding

Hibal Ahmad and Denis Rodrigue *

Department of Chemical Engineering, Université Laval, Quebec City, QC G1V 0A6, Canada; hibal.ahmad.1@ulaval.ca

* Correspondence: denis.rodrigue@gch.ulaval.ca; Tel.: +1-418-656-2903

Abstract: This paper presents a novel recycling approach for porous/foamed crosslinked rotomolded polypropylene (xPP) parts, originally designed for lightweight and thermal insulation. The method uses a cryogenic-assisted shear pulverization technique to produce parts by compression molding. The part's final gel content and crosslink density were found to depend on their dicumyl peroxide (DCP) content (0–2.5 phr) and characterized in terms of their chemical, thermal, physical and mechanical properties. The results show that this recycling technique allows for an effective reprocessing of the crosslinked materials since partial decrosslinking occurs. For example, the crosslink density decreased by 64% (3.10 to 1.11 $\times$ 10^{-3} mol/cm^3) and the gel content by 9% (84.4% to 71.2%) at 2.5 phr DCP. Reprocessing through compression molding led to a compact and partially crosslinked structure resulting in significant improvements in terms of tensile strength (1480%), tensile modulus (604%), elongation at break (8900%), Shore A hardness (19%) and Shore D hardness (32%) compared to xPP samples (at 2.5 phr). This study paves the way for the development of more sustainable recycling methods, especially for crosslinked polymers, by providing new opportunities to reuse the wastes/end-of-life materials in advanced materials and different applications.

Keywords: mechanical recycling; crosslinked polymers; polypropylene; foams; cryogenic treatment; compression molding

Citation: Ahmad, H.; Rodrigue, D. Mechanical Decrosslinking and Reprocessing of Crosslinked Rotomolded Polypropylene Using Cryogenic-Assisted Shear Pulverization and Compression Molding. *Recycling* **2024**, *9*, 129. https://doi.org/10.3390/recycling9060129

Academic Editor: Francesco Paolo La Mantia

Received: 8 November 2024
Revised: 14 December 2024
Accepted: 20 December 2024
Published: 23 December 2024

1. Introduction

Polypropylene (PP) is one of the most widely used thermoplastics, known for its versatility, cost-effectiveness, excellent chemical resistance and good mechanical properties [1–5]. It is extensively used in various industries, including packaging, automotive and consumer goods [6–10]. Despite its widespread applications, conventional polypropylene (PP) is often limited by its thermal properties, especially under harsh conditions (high temperature or prolonged exposure to heat), where its performance can degrade. PP has a melting point at approximately 160–170 °C, and prolonged exposure to elevated temperatures can lead to thermal degradation, reducing its performance. While having acceptable mechanical strength for different applications, its insulation and thermal stability are usually limited for high-performance/extreme environments. To address these limitations, crosslinking techniques have been developed [11–16], transforming PP into a more robust material with a three-dimensional network structure, significantly improving its thermal stability, chemical resistance and overall durability, making it suitable for more demanding applications. For example, xPP is ideal for automotive parts, industrial piping and construction materials where higher heat resistance, chemical exposure and durability are required. Despite its numerous benefits, crosslinked PP (xPP) is seldom used in rigid applications (automotive, aerospace and construction) and very few studies explored this area [17–21].

However, there is growing interest in the development of polymer foams based on xPP. These foams exhibit lightweight characteristics combined with superior thermal and

chemical resistance, making them ideal for applications requiring good insulation, impact resistance and buoyancy [22–25]. The crosslinked structure in xPP foams imparts a unique combination of low density and high performance, which is highly valuable in industries, focusing on material reduction while maintaining functional properties.

Although crosslinking significantly improves the PP's performance, it also introduces some challenges, especially for recycling. Recycling crosslinked polymers, including xPP, is challenging due to their 3D network structure. Unlike thermoplastics, which can be easily recycled and reprocessed by heating above their melting point [26–30], crosslinked polymers are thermosets and conventional recycling techniques cannot directly (re)process them. This limitation makes their recycling difficult and often leads to their disposal in landfills or their burning, both leading to environmental issues. The lack of effective recycling methods for crosslinked polymers highlights a critical gap in the pursuit of sustainable materials and a circular economy.

In response to this challenge, several decrosslinking methods have been developed for crosslinked polymers such as polyethylene (PE): ultrasonic [31,32], chemical [33,34] and mechanochemical [35,36]. While these methods are generally available and show potential at the lab scale, their commercial application for crosslinked PP remains unclear. Nonetheless, more work is necessary as the complexity of crosslinked structures increases, such as highly branched polymers. This is why developing more straightforward and accessible recycling and reprocessing techniques for such complex materials remains a crucial goal for improving the sustainability of crosslinked polymers.

This study aims to address the recycling challenges of xPP by investigating the mechanical recycling of crosslinked rotomolded parts using a novel cryogenic pulverization method. The study focuses on materials produced in our previous work on highly insulative and lightweight xPP produced using a range of dicumyl peroxide (DCP) content (0–2.5 phr) [25]. This variation produced a range of gel content (72.2–80.4%) and crosslink density (1.2–3.1 $\times$ 10^{-3} mol/cm^3). Thus, the main objectives of this study are to evaluate the effect of DCP content on the properties of recycled xPP (r-xPP) and to determine the efficiency of cryogenic pulverization as a viable recycling technique for complex crosslinked polymers. The findings from this research are expected to contribute valuable insights into the development of more sustainable recycling practices for crosslinked materials, advancing the broader field of polymer recycling, especially for complex materials.

2. Results and Discussions

Cryogenic pulverization is a process that cools down the xPP parts to extremely low temperatures (−195 °C), causing their molecular chains to become rigid and brittle. This rigidity reduces chain mobility, making the polymer more susceptible to breaking under mechanical forces (shear and elongation) applied during pulverizing. As a result, the polymer chains undergo partial scission, breaking down into shorter segments and significantly reducing particle size, which is crucial for subsequent reprocessing. Although this process disrupts the tightly crosslinked network (Figure 1b), it does not lead to complete decrosslinking. Some crosslinked segments remain intact, along with new reactive sites and possible weaker associative/dissociative links (Figure 1c). This incomplete crosslinking allows for the formation of a regenerated crosslinked network within the material after compression molding at temperatures above the peak decomposition temperature of DCP (172 °C), as illustrated in Figure 1d. These residual and newly formed links modify the molecular structure and improve the reprocessability of these tightly crosslinked structural materials. Thus, cryogenic pulverization modifies the molecular structure to facilitate recycling, creating finer particles with improved packing, flow and processability while retaining some of the inherent characteristics of the crosslinked xPP, such as gel content (%) and crosslink density (mol/cm^3) as discussed next.

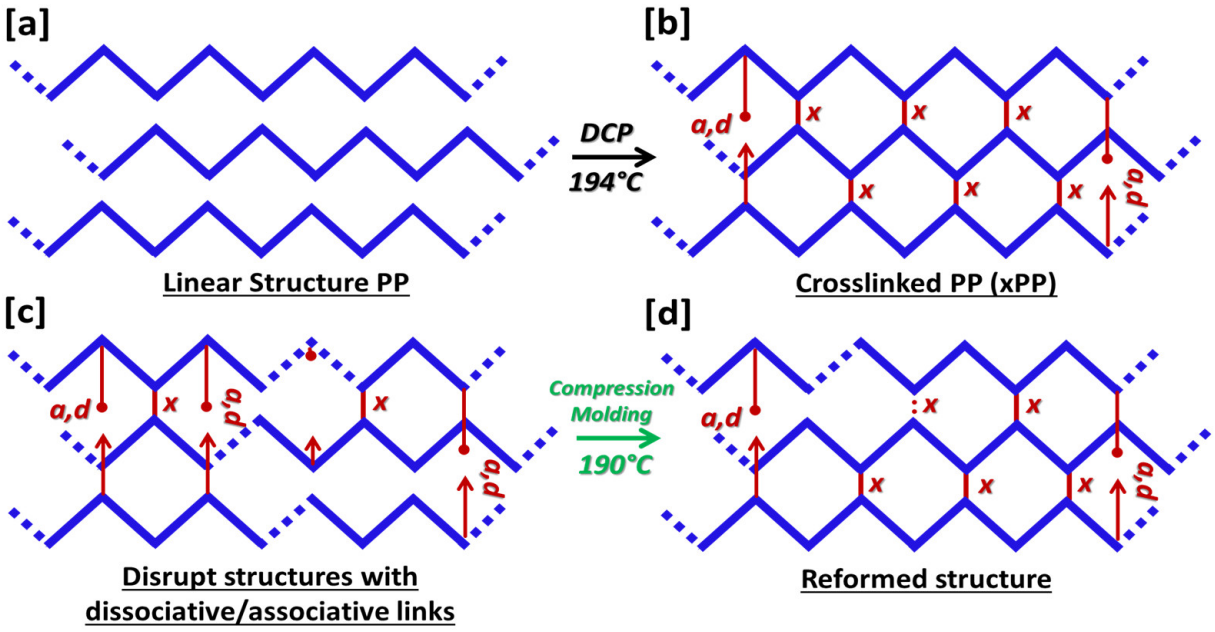

Figure 1. Possible chain mechanisms: (**a**) linear structure, (**b**) crosslinked structure, (**c**) disrupted structure after cryogenic shear pulverization and (**d**) reformed structure after compression molding (x = crosslinked and a,d = associative/dissociative links). Parts in blue are backbone and crosslinks are in red. The arrows refer to position with interaction/reaction.

Figure 2 reports on the gel content and crosslink density of the recycled samples (r-xPP). To understand the effect of cryogenic pulverization and compression molding on the crosslinking efficiency of the samples, the results for xPP samples are also included for comparison. The gel content tends to increase with increasing DCP content (0.5–2.5 phr) for both the original xPP and r-xPP samples. However, the gel content for the r-xPP samples is consistently lower than that of the xPP samples across all DCP concentrations. For instance, at 0.5 phr DCP, the gel content for xPP was 72.2%, while it decreased by 12% to 63.1% for r-xPP. Similarly, at 2.5 phr DCP, the gel content for xPP was 80.4%, which dropped by 9% to 71.2% for r-xPP. Lower values are related to polymer chains in xPP going through thermal and mechanical stresses, leading to partial degradation and break-up of crosslinks (Figure 1), resulting in a lower gel content in r-xPP. Similar trends in gel content reduction were observed in other studies on crosslinked polymers undergoing decrosslinking processes [31,37]. For example, mechanochemical milling of crosslinked low-density polyethylene (XLDPE) reduced the gel content from 62.3% to 14.6% over 20 cycles, mainly through selective chain scission at crosslink points due to mechanical stresses [37]. Similarly, ultrasonic decrosslinking of crosslinked high-density polyethylene (XHDPE) and XLDPE showed significant decreases in gel content attributed to the combined effects of shear stress and acoustic cavitation [31]. These studies highlight the importance of mechanical and ultrasonic forces in disrupting crosslinked networks. However, our study only addresses porous xPP, which has a soft structure compared to the solid-state LDPE and HDPE discussed in the literature. The porous architecture of xPP introduces additional complexities, such as stress distribution within the polymer matrix, which likely influences the efficiency of decrosslinking and subsequent reprocessing.

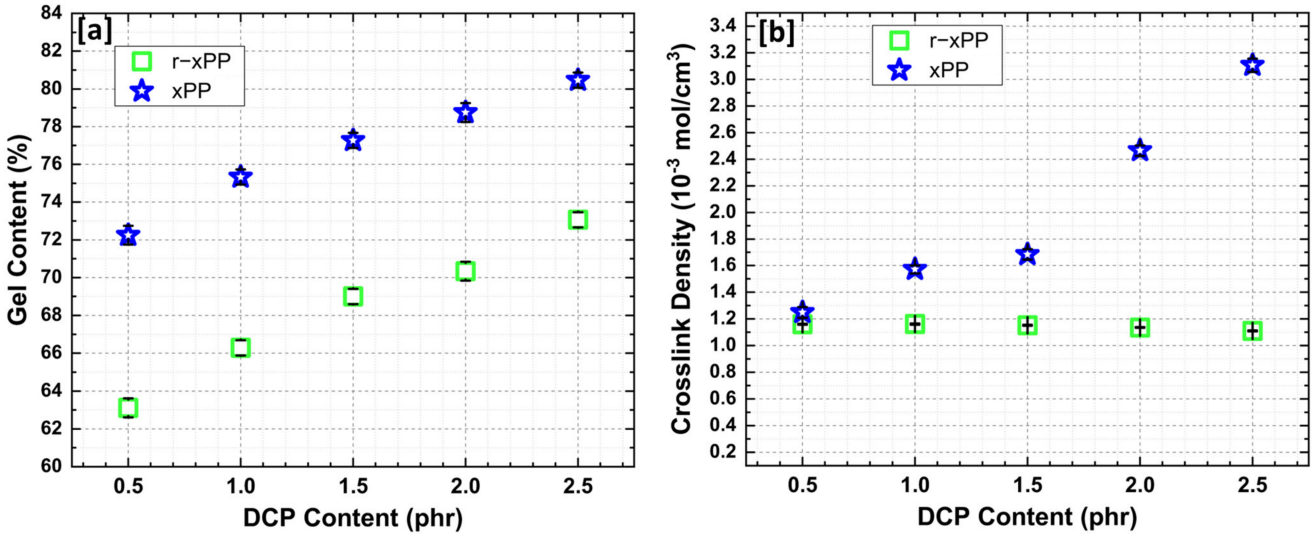

Figure 2. Structural characterization of the crosslinks in xPP [25] and r-xPP samples: (**a**) gel content and (**b**) crosslink density.

Conversely, the crosslink density was found to be lower across all samples in the r-xPP compared to x-PP samples. For example, at 2.5 phr DCP, the crosslink density of the xPP sample was 3.10 × 10^{-3} mol/cm^3, which decreased by 64% (1.11 × 10^{-3} mol/cm^3). When r-xPP is reprocessed with higher DCP content, although more crosslinks are formed, the overall crosslink density still decreases. This is mainly because the recycled material was degraded, resulting in the loss of some crosslinks as observed in studies on the decrosslinking of XHDPE and XLDPE through ultrasonic and mechanochemical methods [31,37,38]. As a result, the new crosslinks formed do not compensate for the crosslinks that were lost during the recycling process. Additionally, cryogenic pulverization can lead to chain scission, breaking polymer chains into smaller segments [35,36]. When these segments are reprocessed during compression molding, they form longer crosslinks with a lower frequency throughout the material. The additional crosslinks formed are not sufficient to fully restore the crosslink density to the levels seen in xPP samples. Despite higher gel content with higher DCP concentrations, the overall crosslink density remains lower in recycled materials due to the residual effects of the previous degradation and the inability to fully re-establish the original crosslinked network. This highlights the importance of cryogenic pulverization in the decrosslinking process, as it enables effective degradation and allows for easier reprocessing, making it a valuable technique for recycling crosslinked materials such as xPP.

Figure 3 presents the FTIR spectra for the selected samples. Typical bands for CH stretching are observed in all of the samples (xPP, rPP, r-xPP) at 2950, 2916 and 2836 cm^{-1}, which correspond to the stretching vibrations of CH_2 and CH_3 groups within the polymer backbone. Additionally, the bands associated with CH_2 deformation and CH_3 symmetric deformation are identified (for all samples) at 1458 and 1378 cm^{-1}, respectively. The C-C backbone bending vibrations are evident at 1170 cm^{-1}, highlighting the structural integrity of the polypropylene chain as reported by Fang et al. [39]. Notably, the presence of a signal at 3380 cm^{-1} is attributed to hydroxyl groups (OH) involved in crosslinking reactions in both xPP and r-xPP samples, indicating potential interactions or modifications within the polymer network [25]. A similar trend for the -OH group was observed at approximately 3417 cm^{-1} and 3400 cm^{-1} by Yasir et al. [12] and Ahmad et al. [11], confirming the presence of a crosslinked structure. Despite these informative spectral features, they are not enough to differentiate between xPP and r-xPP samples. This limitation arises because the FTIR bands mainly reflect the overall molecular structure and functional groups, which may not significantly change during recycling, making it challenging to differentiate between the original (xPP) and recycled (r-xPP) samples based solely on these spectral characteristics.

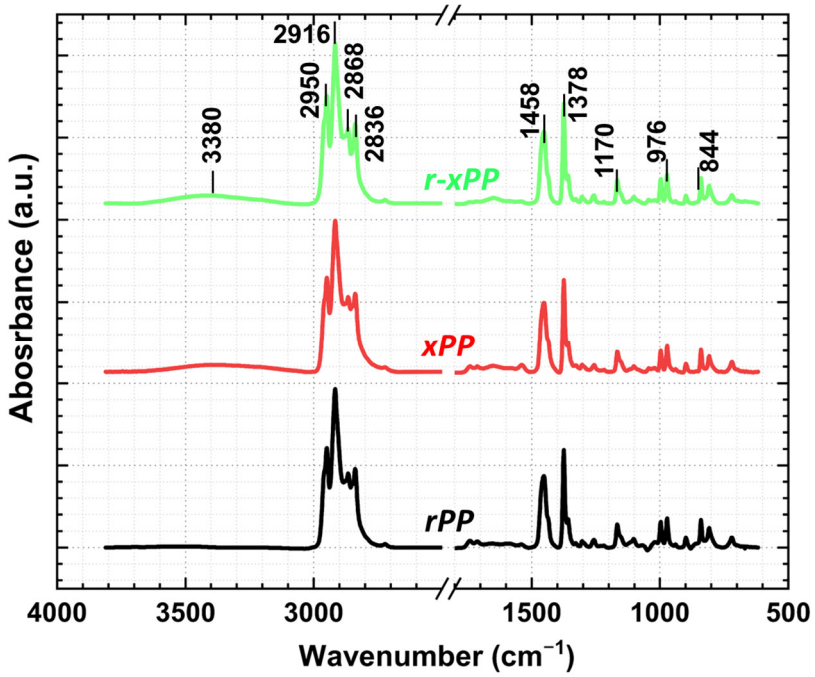

Figure 3. FTIR spectra for typical xPP and rxPP samples at 1.0 phr DCP content.

Table 1 presents the comparative endothermic and exothermic peak information for both r-xPP and xPP with varying DCP (0–2.5 phr) contents. A common trend is observed in both xPP and r-xPP samples, where both the melting temperature and degree of crystallinity decrease with increasing DCP content. This decrease is mainly related to the formation of a crosslinked 3D network, which restricts the mobility of polymer chains, limiting the ability of the material to form more orderly crystalline regions [11,25,31,35]. For example, the melting temperature of recycled PP (rPP) decreases from 163.2 °C to 158.9 °C in the sample originally containing 2.5 phr of DCP (r-xPP). Correspondingly, the degree of crystallinity decreases from 39.1% for rPP to 31.9% for r-xPP with 2.5 phr DCP. Similarly, the neat PP shows a slightly higher melting temperature (165.6 °C) and degree of crystallinity (40.3%) compared to recycled PP (163.2 °C and 39.1%, respectively). This is mainly due to degradation from mechanical stress during recycling, breaking down polymer chains and leading to a lower number of well-ordered crystalline regions.

Table 1. Endothermic and exothermic peak information for r-xPP and xPP [25] samples.

DCP Content (phr)	r-xPP				xPP [25]			
	T_m (°C)	T_c (°C)	Hm (J/g)	X_c (%)	T_m (°C)	T_c (°C)	Hm (J/g)	X_c (%)
0	163.2	127.1	81.0	39.1	165.6	125.4	83.5	40.3
0.5	160.7	122.9	79.3	38.3	160.5	125.4	82.0	39.6
1.0	160.2	122.3	77.2	37.3	158.7	123.6	67.7	32.7
1.5	160.4	120.7	74.1	35.8	156.5	123.2	63.8	30.8
2.0	159.3	120.1	68.3	33.0	153.9	122.2	59.3	28.6
2.5	158.9	118.8	66.0	31.9	153.9	120.9	36.1	17.4

Despite the overall trend, the melting temperature and degree of crystallinity of the r-xPP remain consistently higher than those of the originally crosslinked samples (xPP) at the same DCP content. For example, at 2.5 phr DCP, the melting temperature (158.9 °C) and degree of crystallinity (31.9%) of the r-xPP sample are significantly higher than those of the corresponding xPP (153.9 °C and 17.4%, respectively). This difference in thermal behavior can be attributed to the different processing methods used for the xPP (rotational

molding) and r-xPP (compression molding) samples and cryogenic pulverization. For xPP samples produced via rotational molding, higher DCP content results in a foamed or porous structure leading to more voids and defects contributing to a more amorphous and thinner cell wall (more bubbles) structure. This, in turn, significantly reduces the crystallinity and melting temperature [25]. In contrast, the r-xPP, produced through compression molding, experiences continuous heating and is subjected to high pressure (2.5 tons). The faster water-cooling used in this process enhances crystallization compared to the slower air cooling used in rotational molding. This combination of high pressure and fast cooling allows for the trapped bubbles to escape, resulting in a denser and more ordered structure with fewer defects, ultimately improving the thermal properties (melting and crystallization) of r-xPP. Furthermore, cryogenic pulverization also breaks the crosslink structure and improves the mobility of polymer chain segments during the crystallization process, as mentioned by Hejun et al. [35], leading to a higher degree of crystallinity for r-xPP samples.

Figure 4 reports on the density of the r-xPP samples compared to the xPP ones, where the latter exhibits a significantly lower density. For instance, the density of xPP with 2.5 phr DCP is 0.378 g/cm^3, while r-xPP exhibits a density of 0.894 g/cm^3, an increase of 136%. This difference arises from the different manufacturing methods: rotomolding used for xPP results in a porous material due to the absence of applied pressure and rapid solidification (less time available for gas bubbles to escape), leading to bubble entrapment, while compression molding used for r-xPP applies pressure, compacting the material and eliminating bubble formation, leading to a denser structure [3]. Despite the overall increase in density after recycling, the density of r-xPP decreases with higher DCP content due to the partial degradation of crosslinked networks during recycling, modifying the final density.

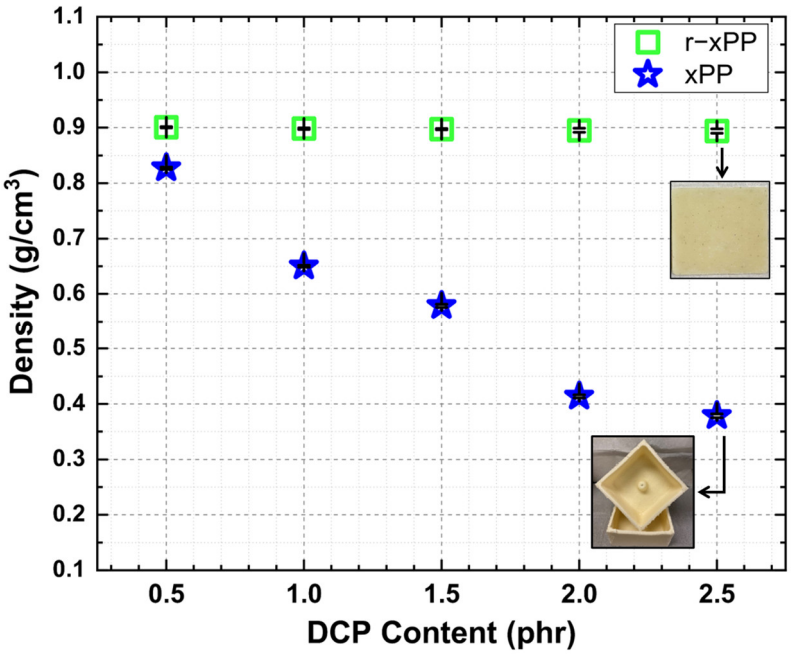

Figure 4. Density of the xPP and r-xPP [25] samples.

The temperature-dependent thermal conductivity of the r-xPP samples is shown in Figure 5. The thermal conductivity decreases with increasing DCP content in r-xPP. The value decreases by 19% (from 0.154 W/m.K (rPP) to 0.125 W/m.K (2.5 phr)) at room temperature (23 °C). On the other hand, the thermal resistance increases by 17% (0.216–0.253 K/W) as stated in Table 2. These changes are caused by the 3D network structure, limiting the mobility of molecules and slowing down the heat transfer within the material, as explained in our previous work on crosslinked polymers (PE) [11,14]. Additionally, chain scission from cryogenic pulverization generates shorter segments that further impair thermal transport properties. However, as the temperature increases from 23 °C (Figure 5a) to 120 °C

(Figure 5f), the thermal conductivity also increases by 12% for rPP (0.154–0.173 W/m.K) and 17% for 2.5 phr DCP content r-xPP (0.126–0.146 W/m.K). This is because the mobility of polymer chains improves with increasing temperature, thus improving heat transfer through molecular mobility [25]. As expected, the xPP samples exhibit lower thermal conductivity over the whole DCP concentration range, again due to the manufacturing method used (rotomolding) generating a porous structure with more bubbles (thermal insulators) to reduce heat transfer [25]. While no studies have directly examined the thermal conductivity as a function of temperature in crosslinked polymers, our findings reveal that crosslinking and reprocessing conditions significantly affect the thermal transport properties of recycled materials. This highlights the potential of cryogenic pulverization to tailor the thermal properties, which is an opportunity for further research and application development.

Table 2. Temperature-dependent thermal resistivity (*R*) with their standard deviation for the r-xPP samples.

DCP Content (phr)	23 °C (K/W)	40 °C (K/W)	60 °C (K/W)	80 °C (K/W)	100 °C (K/W)	120 °C (K/W)
0 (rPP)	0.0216 (0.0001)	0.0210 (0.0001)	0.0208 (0.0001)	0.0204 (0.0001)	0.0199 (0.0001)	0.0192 (0.0001)
0.5	0.0223 (0.0001)	0.0218 (0.0001)	0.0209 (0.0001)	0.0205 (0.0001)	0.0200 (0.0001)	0.0193 (0.0001)
1.0	0.0227 (0.0001)	0.0220 (0.0001)	0.0213 (0.0001)	0.0210 (0.0001)	0.0208 (0.0001)	0.0204 (0.0001)
1.5	0.0239 (0.0001)	0.0234 (0.0001)	0.0223 (0.0001)	0.0221 (0.0001)	0.0214 (0.0001)	0.0208 (0.0001)
2.0	0.0250 (0.0001)	0.0247 (0.0001)	0.0230 (0.0001)	0.0227 (0.0001)	0.0226 (0.0001)	0.0219 (0.0001)
2.5	0.0253 (0.0001)	0.0249 (0.0001)	0.0236 (0.0001)	0.0231 (0.0001)	0.0227 (0.0001)	0.0223 (0.0001)

Figure 6 shows the mechanical properties of the r-xPP. The same decreasing trends are observed for the tensile strength (Figure 6a), modulus (Figure 6b), elongation at break (Figure 6c) and hardness (Figure 6d) of the r-xPP with increasing DCP content. For instance, the tensile strength (56%), modulus (24%), Shore A (6 points) and Shore D (14 points) decreased with 2.5 phr DCP. This is because increasing the crosslinking (gel content) reduced the crystallinity (Table 1), leading to a more brittle material. As the DCP content increases, the gel content also increases while the crosslink density decreases (for recycled samples), resulting in a complex network with lower load-bearing capabilities. Additionally, the presence of voids and the disruption of polymer chain continuity during recycling further compromise the mechanical integrity, leading to lower tensile strength and modulus. However, these properties were found to be higher than those for rotomolded xPP [25], except for rPP, for which the values decrease due to mechanical degradation. Nevertheless, the mechanical properties are higher for r-xPP samples at higher DCP content. For example, the tensile strength (1480%), tensile modulus (604%), elongation at break (8900%), Shore A (19%) and Shore D (32%) increased at 2.5 phr DCP for r-xPP as presented in Tables 3 and 4. These improvements are significantly higher compared to other studies on decrosslinking [31,32,38,40,41], owing to the unique use of crosslinked, rotomolded and porous polypropylene (xPP) [25], as well as the combined effects of cryogenic pulverization and compression molding. Cryogenic pulverization generates chain scission, breaking polymer chains into shorter segments, which are then rearranged and aligned during compression molding under high pressure. This process promotes better packing and alignment of polymer chains, resulting in a denser and more robust material. In contrast, the foam-like structure from rotational molding introduces more variability in mechanical properties, making recycled xPP from compression molding more mechanically stable, despite its challenges [3].

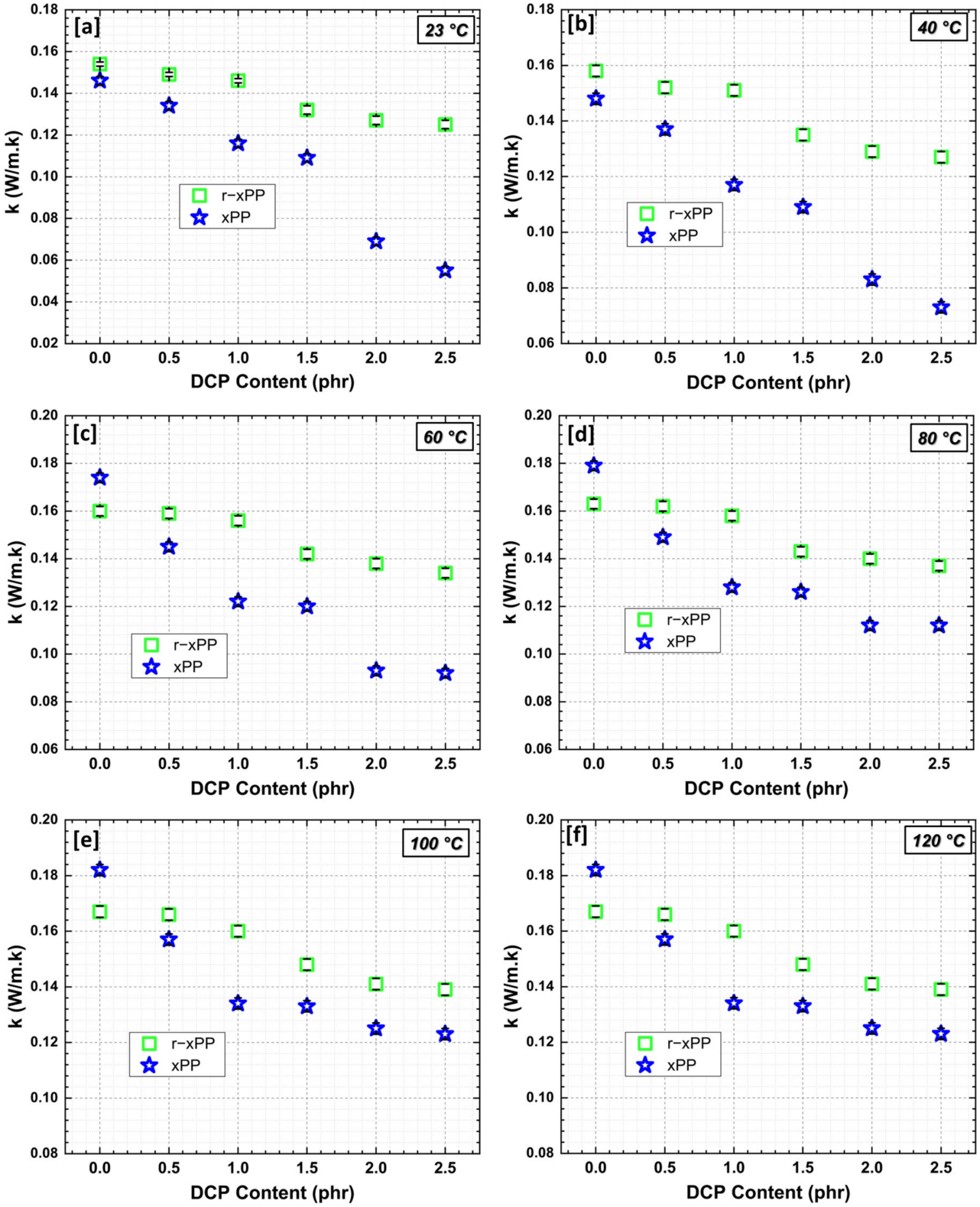

Figure 5. Temperature-dependent thermal conductivity of the x-PP [25] and r-xPP samples at: (**a**) 23, (**b**) 40, (**c**) 60, (**d**) 80, (**e**) 100 and (**f**) 120 °C.

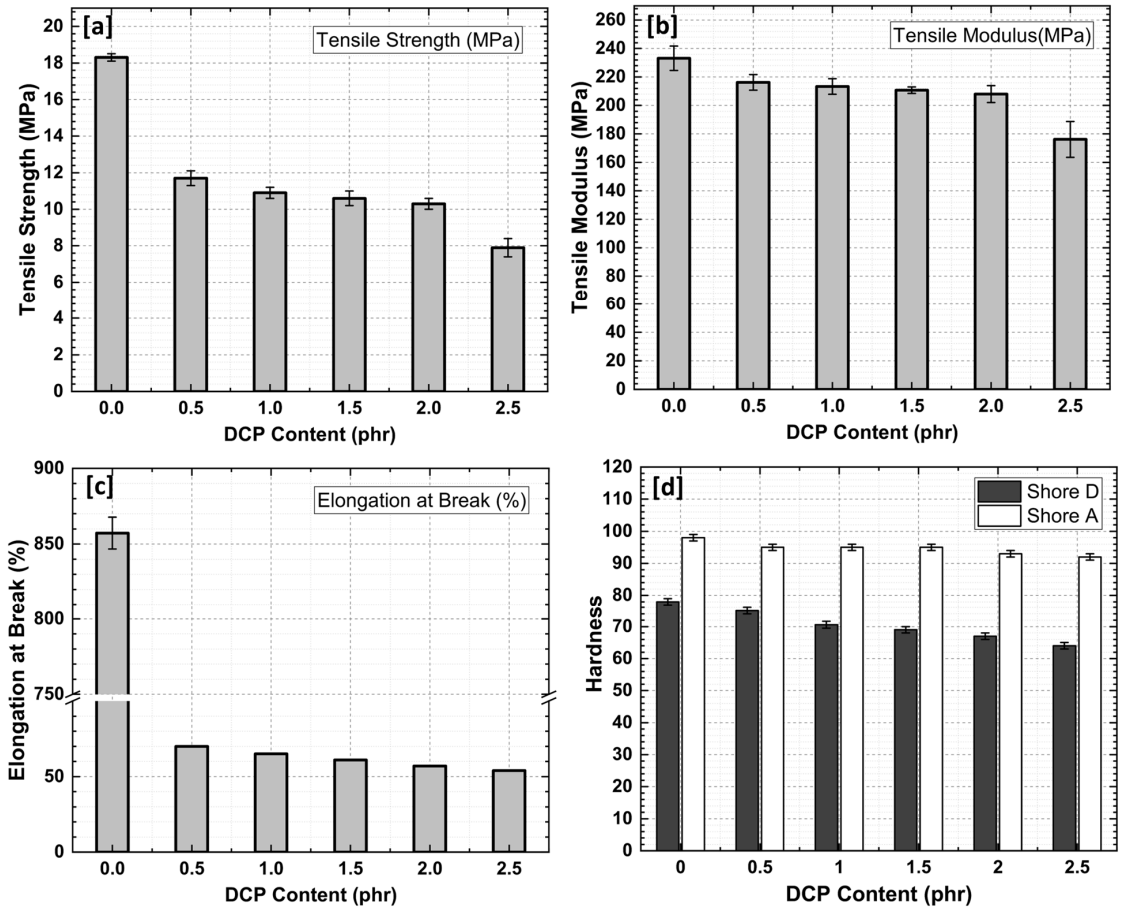

Figure 6. Mechanical properties of the r-xPP samples: (**a**) tensile strength, (**b**) tensile modulus, (**c**) elongation at break and (**d**) hardness (Shore A and D).

Table 3. Tensile properties of r-xPP and xPP as a function of DCP content.

DCP Content (phr)	Tensile Strength (MPa)		Tensile Modulus (MPa)		Elongation at Break (%)	
	r-xPP	xPP [25]	r-xPP	xPP [25]	r-xPP	xPP [25]
0	18.3 (0.2)	18.8 (0.7)	233 (19)	282 (47)	857 (11)	95 (16)
0.5	11.7 (0.1)	10.9 (0.8)	216 (6)	190 (31)	70 (1)	16.4 (0.4)
1.0	10.9 (0.3)	4.3 (0.5)	213 (6)	158 (24)	52 (1)	10.8 (0.4)
1.5	10.6 (0.4)	2.7 (0.6)	211 (2)	94 (32)	61 (1)	0.70 (0.01)
2.0	10.3 (0.3)	1.1 (0.2)	208 (6)	58 (1)	70 (1)	0.60 (0.05)
2.5	7.9 (1.5)	0.5 (0.1)	176 (13)	25 (1)	54 (1)	0.60 (0.05)

Table 4. Hardness (Shore A and D) of the r-xPP and xPP samples as a function of DCP content.

DCP Content (phr)	Hardness (Shore A)		Hardness (Shore D)	
	r-xPP	xPP [25]	r-xPP	xPP [25]
0	98 (1)	93 (1)	78 (1)	73 (1)
0.5	95 (1)	89 (1)	75 (1)	65 (1)
1.0	95 (1)	85 (1)	71 (1)	64 (1)
1.5	95 (1)	82 (1)	69 (1)	63 (1)
2.0	93 (1)	79 (1)	67 (1)	59 (1)
2.5	92 (1)	77 (1)	64 (1)	49 (1)

3. Materials and Methods

The materials used in this study are based on our previous research [25], where polypropylene (PP, RMPP141 NATURAL from Rotoworx) with a melt flow index of 13 g/10 min (2.16 kg/230 °C) and a density of 0.902 g/cm^3 was crosslinked using dicumyl peroxide (DCP) with various contents (0–2.5 phr) to produce lightweight, thermally insulative and crosslinked porous parts (xPP) using rotational molding (oven temperature of 194 °C, oven time of 30 min, cooling time of 25 min, and arm-to-plate rotation of 5:1 rpm). Additionally, Irganox 1076 antioxidant (BASF, USA) was incorporated to prevent oxidative degradation and was used as received. The samples were characterized by their gel content and crosslink density, determined using the method described in Section 3.2, which are the main parameters of crosslinked polymer structures, as summarized in Table 5. Moreover, xylene and toluene were used as received from Fisher Chemicals (USA) for solvent extraction and equilibrium swelling methods, respectively. For recycling, liquid nitrogen (N_2) from Praxair (Canada) was used.

Table 5. Gel content and crosslink density as a function of DCP content [25].

DCP Content (phr)	Antioxidant (phr)	Gel Content (%)	Crosslink Density (10^{-3} mol/cm^3)
0	0.15	-	-
0.5	0.15	72.2 (0.5)	1.24 (0.04)
1.0	0.15	75.3 (0.4)	1.57 (0.03)
1.5	0.15	77.2 (0.4)	1.68 (0.04)
2.0	0.15	78.7 (0.5)	2.46 (0.04)
2.5	0.15	80.4 (0.4)	3.10 (0.05)

3.1. Recycling and Reprocessing of Crosslinked Rotomolded Parts

Despite the inherent challenges related to their crosslinked structure, recycling crosslinked parts is crucial for minimizing waste and promoting a more circular economy within the plastics industry. After their characterization (Table 5), the rotomolded xPP parts were individually crushed and ground in a laboratory-scale grinder (Retsch, SM 2000, Haan Germany) to produce pellets approximately 0.5–1 cm in size, as depicted in Figure 7. Subsequently, the materials underwent cryogenic treatment using liquid nitrogen (−195 °C). This low-temperature treatment is necessary to decrease the toughness of the crosslinked polymer, making it more amenable to mechanical processing (crushing and grinding) and potentially helping its decrosslinking. After cryogenic treatment, the materials were pulverized using a lab mill model PKA-18 (Powder King, Phoenix, AZ, USA). This pulverizer features eight grinding disks applying high shear forces to break down the materials into fine particles. The system includes thermocouples to monitor the temperature and a mechanism to control the material flow rate. The system was run at a constant temperature (60 °C), ensuring both material integrity and equipment safety. The cryogenic step also improves the ability of shear forces during pulverization to break down the tough, crosslinked structure of xPP. Using liquid nitrogen maintains stable temperatures during pulverization, and this cooling effect allows the disks to efficiently process the material without overheating, improving the overall efficiency and safety of the operation. Finally, the particles were sieved using a mesh sieve with an opening of 1 mm to keep only particle sizes of less than 1 mm, as shown in Figure 8.

Figure 8 also compares the materials that did not undergo cryogenic treatment and optical microscopy images (VHX Keyence, Canada) for the sieved particles. Recycling xPP without cryogenic treatment was difficult due to its high toughness, possibly leading to equipment damage. In contrast, the cryogenically treated samples showed significantly improved grindability (Figure 8c,d), confirming the method's efficiency in improving the recyclability of crosslinked polymers.

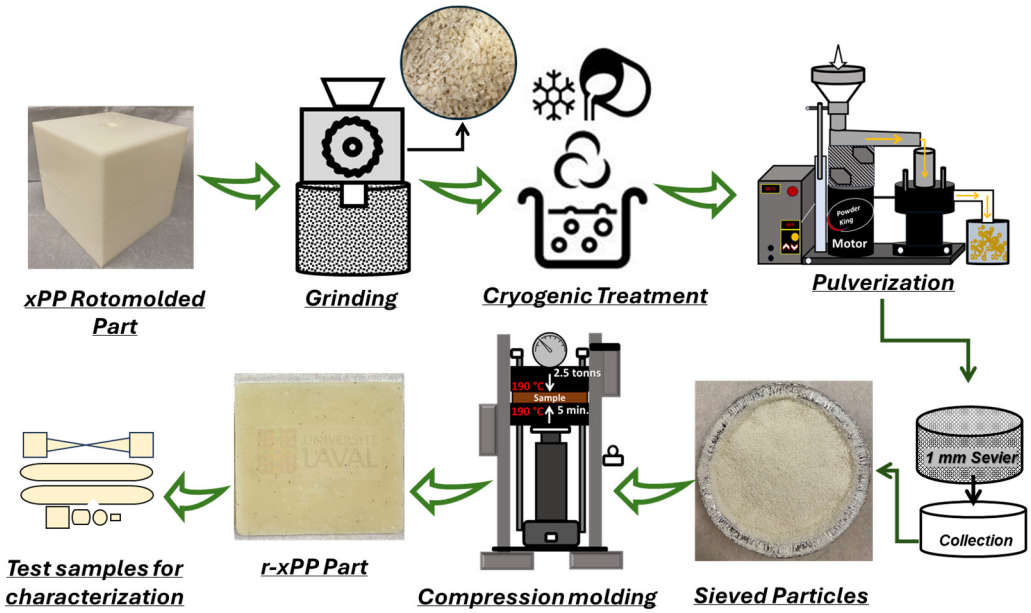

Figure 7. Schematic representation of the step-by-step process for recycling xPP parts using cryogenic pulverization and compression molding.

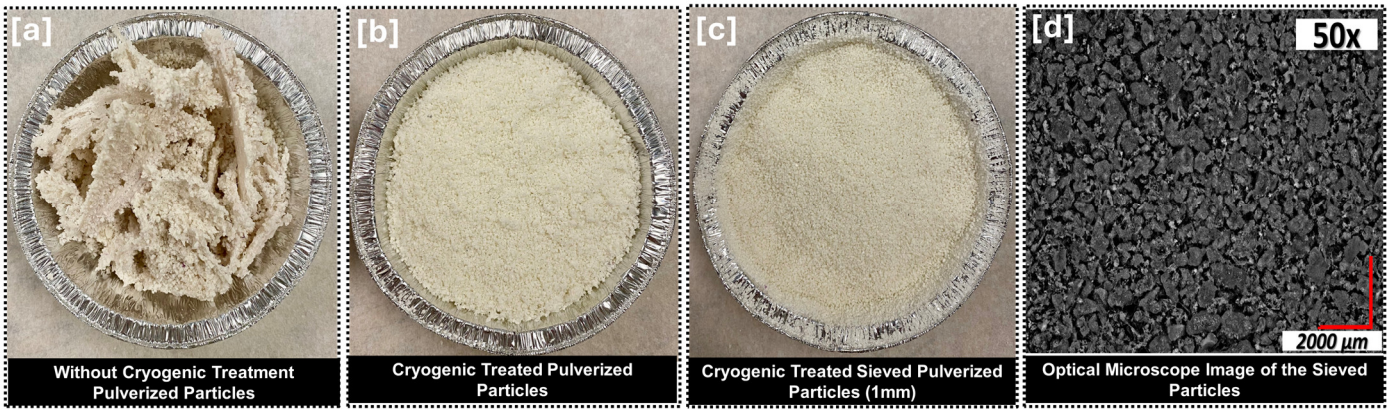

Figure 8. Particles obtained: (**a**) without cryogenic treatment, (**b**) with cryogenic treatment, (**c**) sieved (1 mm) and (**d**) surface topology of the sieved particles (optical microscopy at 50×).

As a first step (proof of concept), the sieved particles (100%) were reprocessed through compression molding (Carver Press C, Wabash, IN, USA) using a stainless steel mold (102 × 102 × 3.4 mm^3) following a specific procedure: preheating at 190 °C for 3 min, applying a force of 2.5 tons for 5 min and subsequently cooling under pressure to 60 °C using circulating water. Compression molding was chosen due to its ability to apply uniform pressure and heat, allowing for better packing and alignment of polymer chains. This method not only enables the reuse of the crosslinked xPP, but also addresses the challenges associated with recycling thermoset materials, promoting sustainability in the production of polymer-based products. For comparison, neat rotomolded PP parts were also recycled with the same processing conditions. This involved subjecting the PP parts to the same cryogenic pulverization and compression molding process. Typical examples of recycled PP (rPP) and r-xPP parts that were initially crosslinked with various DCP contents (0.5, 1.0, 1.5, 2.0 and 2.5 phr) during the original rotomolding process (as detailed in Table 5) are shown in Figure 9. Although the DCP content influences the thickness of the original parts due to the porous structure created by crosslinking, the r-xPP samples did not exhibit noticeable differences in thickness and/or color after recycling (compact structure). The parts were then cut into different geometries for characterization.

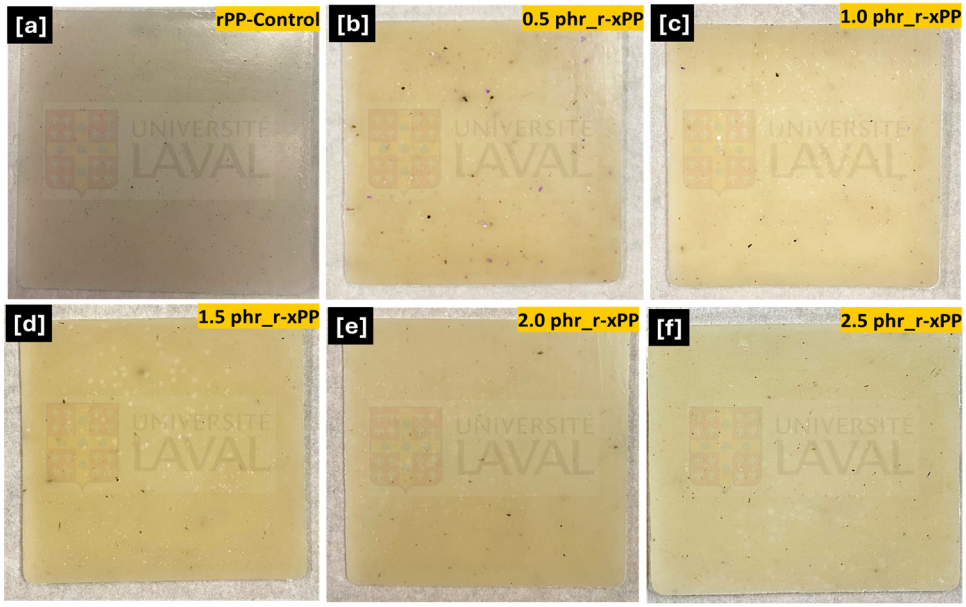

Figure 9. Typical images of the recycled PP and xPP parts: (**a**) rPP, (**b**) 0.5, (**c**) 1.0, (**d**) 1.5, (**e**) 2.0 and (**f**) 2.5 phr r-xPP. The numbers represent the DCP content in the original samples.

3.2. Characterization

To determine the effect of recycling on the crosslinking efficiency, the gel content of the recycled parts was measured using the Soxhlet extraction method (ASTM D2765-16) [42]. Approximately 0.2–0.3 g of the sample was placed in a preweighed stainless steel mesh pouch and refluxed in xylene for 12 h at 140 °C. After extraction, the samples were oven-dried at 85 °C for 6 h until a constant weight was achieved. The gel fraction (C_{gel}) was calculated from three replicates by determining the ratio of the weight of the insoluble polymer to the initial sample weight as:

$$C_{gel}(\%) = \frac{W_f}{W_i}\,(100), \tag{1}$$

where W_f is the final weight after extraction and drying, and W_i is the initial weight of the samples.

The crosslink density was evaluated using the equilibrium swelling method (ASTM D6814-02) [43]. Specimens weighing 5–10 g were immersed in toluene for 72 h, after which the swollen weight (*ms*) was recorded. The samples were then dried overnight at 85 °C and weighed again to determine the dry weight (*mr*). This procedure was repeated three times for each sample. The crosslink density was then calculated using the Flory–Rehner equation [25,44]:

$$v_e = \frac{-\left[ln(1-V_r) + V_r + X\,V_r^2\right]}{V_1\left(V_r^{\frac{1}{3}} - \frac{1}{2}V_r\right)} \tag{2}$$

where v_e is the crosslink density (mol/cm^3), V_1 is the solvent molar volume (106.2 cm^3/mol for toluene), X is the polymer-solvent interaction parameter (0.391), and V_r is the gel volume in the swollen sample calculated as:

$$V_r = \frac{\frac{m_r}{\rho_r}}{\frac{m_r}{\rho_r} + \frac{m_s}{\rho_s}} \tag{3}$$

where ρ_r is the density of the dry samples and ρ_s is the solvent density (0.867 g/cm^3).

Fourier transform infrared (FTIR) analysis was conducted to identify the characteristic peaks of the neat and recycled parts. The analysis was performed using a nitrogen-purged

FTIR spectrometer (Nicolet iS50, Thermo Fisher Scientific, Waltham, MA, USA) equipped with a KBr beam splitter and an MCT detector cooled by nitrogen. The spectra were recorded over a range of 3500–500 cm^{-1}. Each spectrum represents an average of 128 scans at a resolution of 4 cm^{-1}.

The melting and crystallization behavior was assessed using differential scanning calorimetry (DSC 25, TA Instruments, New Castle, DE, USA). Each sample (5–10 mg) was placed in an aluminum pan. The analysis consisted of heating the sample from 20 to 180 °C at a rate of 10 °C/min in a nitrogen atmosphere, followed by cooling back to 20 °C at the same rate. The degree of crystallinity (X_c) for xPP was calculated as:

$$X_c(\%) = \frac{\Delta H_m}{\Delta H_{m0}}(100) \quad (4)$$

where ΔHm_0 represents the melting enthalpy of 100% crystalline PP, which is 207 J/g [45].

A homemade thermal conductivity analyzer, based on ASTM E1225-20 [46], was used to determine the temperature-dependent thermal conductivity across a temperature range (23–120 °C). The samples were cut into 50 × 50 mm^2 pieces, and their thickness was measured with a digital caliper (Mastercraft, Toronto, Canada). The analyzer's upper (heating) and lower (cooling) plates were maintained at a 20 °C temperature difference (ΔT), with the plates set to average temperatures of 23, 40, 60, 80, 100 and 120 °C. Each sample was placed between thin aluminum sheets to reduce thermal contact resistance. The thermal conductivity was calculated using Fourier's law as:

$$k = \frac{Q\,L}{\Delta T} \quad (5)$$

where Q is the heat flux and L is the sample thickness. The average and standard deviation were obtained from three repetitions. More information can be obtained from previous studies [11,14].

The thermal resistivity (R) was calculated as:

$$R = \frac{L}{k} \quad (6)$$

Tensile tests were conducted on an Instron universal testing machine (model 5565, Instron, Norwood, MA, USA) with a 500 N load cell (ASTM D638-22, type V) [47] at a constant crosshead speed of 10 mm/min. The tensile modulus, strength and elongation at break were calculated by averaging results from at least four specimens, including standard deviations.

The surface hardness was measured using a model 306 L (Shore A) and model 307 L (Shore D) durometer (PTC Instruments, Los Angeles, CA, USA) to assess the softness/flexibility and hardness of the samples, respectively, according to ASTM D2240-15 [48]. Five measurements were taken for each sample (50 × 50 mm^2) on each side (internal and external) to report averages and standard deviations.

4. Conclusions

This study proposed an innovative recycling approach for porous/foamed crosslinked rotomolded polypropylene (xPP) parts using a cryogenic-assisted shear pulverization technique followed by compression molding. The method not only enabled the recycling of crosslinked xPP materials, but also resulted in partial decrosslinking, with a significant reduction in crosslink density (64%) and gel content (9%) at higher DCP content (2.5 phr). The reprocessed samples exhibited a compact and partially crosslinked structure, leading to substantial improvements in mechanical properties, including tensile strength (1480%), tensile modulus (604%), elongation at break (8900%) and hardness (19% for Shore A and 32% for Shore D).

These findings highlight the potential of this recycling technique to enhance the performance of crosslinked polypropylene, transforming the materials into more valuable parts suitable for demanding applications such as automotive, construction and high-performance commercial/industrial components. This approach offers a sustainable and efficient solution to the challenges of recycling crosslinked polymers, promoting their use in advanced engineering fields and industries, including aerospace, consumer goods, construction materials and electronics.

Moreover, the successful application of cryogenic pulverization followed by compression molding offered significant advantages in terms of material recovery and processing efficiency. By decrosslinking the polymer and improving its mechanical properties, this technique made recycled PP a viable material for various high-performance applications (automotive, aerospace, construction, etc.), contributing to waste reduction and sustainability efforts in the polymer industry.

Finally, future work should focus on optimizing the methods and processing conditions while extending the concept to other crosslinked polymers (polyethylene, polyamides, etc.), further contributing to sustainable material development and waste reduction efforts in the polymer industry. Additionally, research should evaluate the scalability and economic feasibility of the proposed method, exploring its potential for industrial-scale applications. This will help to bridge the gap between laboratory innovation and real-world implementation, ensuring a broader impact across various sectors.

Author Contributions: Conceptualization, H.A. and D.R.; methodology, H.A.; validation, H.A. and D.R.; formal analysis, H.A.; investigation, H.A.; resources, D.R.; data curation, H.A. and D.R.; writing—original draft preparation, H.A.; writing—review and editing, H.A. and D.R.; visualization, H.A. and D.R.; supervision, D.R.; project administration, D.R.; funding acquisition, D.R. All authors have read and agreed to the published version of the manuscript.

Funding: This research was funded by the Association of Rotational Molders (ARM), via the Crawford Education and Development Foundation.

Data Availability Statement: The original contributions presented in this study are included in the article. Further inquiries can be directed to the corresponding author.

Acknowledgments: The authors thank Rotoworx for providing the polypropylene samples.

Conflicts of Interest: The authors declare no conflicts of interest.

References

1. Shubhra, Q.T.H.; Alam, A.; Quaiyyum, M.A. Mechanical Properties of Polypropylene Composites: A Review. *J. Thermoplast. Compos. Mater.* **2011**, *26*, 362–391. [CrossRef]
2. Grebowicz, J.; Lau, S.-F.; Wunderlich, B. The Thermal Properties of Polypropylene. *J. Polym. Sci. Polym. Symp.* **1984**, *71*, 19–37. [CrossRef]
3. Dou, Y.; Rodrigue, D. Morphological, Thermal and Mechanical Properties of Polypropylene Foams via Rotational Molding. *Cell. Polym.* **2021**, *40*, 198–211. [CrossRef]
4. Akinci, A.; Akbulut, H.; Yilmaz, F. Mechanical Properties of Cost-Effective Polypropylene Composites Filled with Red-Mud Particles. *Polym. Polym. Compos.* **2008**, *16*, 439–446. [CrossRef]
5. Hussein, T.A.; Dheyaaldin, M.H.; Mosaberpanah, M.A.; Ahmed, Y.M.S.; Mohammed, H.A.; Omer, R.R.; Hamid, S.M.; Alzeebaree, R. Chemical Resistance of Alkali-Activated Mortar with Nano Silica and Polypropylene Fiber. *Constr. Build. Mater.* **2023**, *363*, 129847. [CrossRef]
6. Moritomi, S.; Watanabe, T.; Kanzaki, S. Polypropylene Compounds for Automotive Applications. *Sumitomo Kagaku* **2010**, *1*, 1–16.
7. Hariprasad, K.; Ravichandran, K.; Jayaseelan, V.; Muthuramalingam, T. Acoustic and Mechanical Characterisation of Polypropylene Composites Reinforced by Natural Fibres for Automotive Applications. *J. Mater. Res. Technol.* **2020**, *9*, 14029–14035. [CrossRef]
8. Hossain, M.T.; Shahid, M.A.; Mahmud, N.; Habib, A.; Rana, M.M.; Khan, S.A.; Hossain, M.D. Research and Application of Polypropylene: A Review. *Discov. Nano* **2024**, *19*, 2. [CrossRef]
9. Ayhan, Z.; Cimmino, S.; Esturk, O.; Duraccio, D.; Pezzuto, M.; Silvestre, C. Development of Films of Novel Polypropylene Based Nanomaterials for Food Packaging Application. *Packag. Technol. Sci.* **2015**, *28*, 589–602. [CrossRef]

10. Mallick, P.K. Chapter 5—Thermoplastics and Thermoplastic–Matrix Composites for Lightweight Automotive Structures. In *Woodhead Publishing in Materials*; Mallick Design and Manufacturing for Lightweight Vehicles (Second Edition); Woodhead Publishing: Sawston, UK, 2021; pp. 187–228; ISBN 978-0-12-818712-8.
11. Ahmad, H.; Rostami-Tapeh-Esmaeil, E.; Rodrigue, D. The Effect of Chemical Crosslinking on the Properties of Rotomolded High Density Polyethylene. *J. Appl. Polym. Sci.* **2024**, *141*, e54744. [CrossRef]
12. Gill, Y.Q.; Ehsan, H.; Mehmood, U.; Irfan, M.S.; Saeed, F. A Novel Two-Step Melt Blending Method to Prepare Nano-Silanized-Silica Reinforced Crosslinked Polyethylene (XLPE) Nanocomposites. *Polym. Bull.* **2022**, *79*, 10077–10093. [CrossRef]
13. Sirisinha, K.; Boonkongkaew, M.; Kositchaiyong, S. The Effect of Silane Carriers on Silane Grafting of High-Density Polyethylene and Properties of Crosslinked Products. *Polym. Test.* **2010**, *29*, 958–965. [CrossRef]
14. Mathews, C.L.; Wasel, O.; Isaacson, K.P.; Proctor, C.R.; Tariq, M.; Shah, A.D.; Freeman, J.L.; Whelton, A.J. Crosslinked Polyethylene (PEX) Drinking Water Pipe: Carbon Leaching, Impacts on Microbial Growth, and Developmental Toxicity to Zebrafish. *Environ. Adv.* **2023**, *13*, 100386. [CrossRef]
15. Ahmad, H.; Rodrigue, D. Crosslinked Polyethylene: A Review on the Crosslinking Techniques, Manufacturing Methods, Applications, and Recycling. *Polym. Eng. Sci.* **2022**, *62*, 2376–2401. [CrossRef]
16. Kaltenegger-Uray, A.; Rieß, G.; Lucyshyn, T.; Holzer, C.; Kern, W. Physical Foaming and Crosslinking of Polyethylene with Modified Talcum. *Polymers* **2019**, *11*, 1472. [CrossRef]
17. Yu, Q.; Zhu, S. Peroxide Crosslinking of Isotactic and Syndiotactic Polypropylene. *Polymer* **1999**, *40*, 2961–2968. [CrossRef]
18. Yuan, M.; Zhang, G.; Li, B.; Chung, T.C.M.; Rajagopalan, R.; Lanagan, M.T. Thermally Stable Low-Loss Polymer Dielectrics Enabled by Attaching Cross-Linkable Antioxidant to Polypropylene. *ACS Appl. Mater. Interfaces* **2020**, *12*, 14154–14164. [CrossRef]
19. Beltraán, M.; Mijangos, C. Silane Grafting and Moisture Crosslinking of Polypropylene. *Polym. Eng. Sci.* **2000**, *40*, 1534–1541. [CrossRef]
20. Sawasaki, T.; Nojiri, A. Radiation Crosslinking of Polypropylene. *Int. J. Radiat. Appl. Instrumentation. Part C Radiat. Phys. Chem.* **1988**, *31*, 877–886. [CrossRef]
21. Yoshiga, A.; Otaguro, H.; Parra, D.F.; Lima, L.F.C.P.; Lugao, A.B. Controlled Degradation and Crosslinking of Polypropylene Induced by Gamma Radiation and Acetylene. *Polym. Bull.* **2009**, *63*, 397–409. [CrossRef]
22. Liu, H.; Chuai, C.; Iqbal, M.; Wang, H.; Kalsoom, B.B.; Khattak, M.; Qasim Khattak, M. Improving Foam Ability of Polypropylene by Crosslinking. *J. Appl. Polym. Sci.* **2011**, *122*, 973–980. [CrossRef]
23. Zhai, W.; Wang, H.; Yu, J.; Dong, J.; He, J. Cell Coalescence Suppressed by Crosslinking Structure in Polypropylene Microcellular Foaming. *Polym. Eng. Sci.* **2008**, *48*, 1312–1321. [CrossRef]
24. Yang, C.; Xing, Z.; Zhao, Q.; Wang, M.; Wu, G. A Strategy for the Preparation of Closed-Cell and Crosslinked Polypropylene Foam by Supercritical CO_2 Foaming. *J. Appl. Polym. Sci.* **2018**, *135*, 45809. [CrossRef]
25. Ahmad, H.; Rodrigue, D. Development of Lightweight and Thermally Insulative Crosslinked Polypropylene via Rotomolding. *Polym. Eng. Sci.* **2024**. Submitted.
26. Lamtai, A.; Elkoun, S.; Robert, M.; Mighri, F.; Diez, C. Mechanical Recycling of Thermoplastics: A Review of Key Issues. *Waste* **2023**, *1*, 860–883. [CrossRef]
27. Podara, C.; Termine, S.; Modestou, M.; Semitekolos, D.; Tsirogiannis, C.; Karamitrou, M.; Trompeta, A.-F.; Milickovic, T.K.; Charitidis, C. Recent Trends of Recycling and Upcycling of Polymers and Composites: A Comprehensive Review. *Recycling* **2024**, *9*, 37. [CrossRef]
28. Benoit, N.; González-Núñez, R.; Rodrigue, D. Long-Term Closed-Loop Recycling of High-Density Polyethylene/Flax Composites. *Prog. Rubber Plast. Recycl. Technol.* **2018**, *34*, 171–199. [CrossRef]
29. Oladele, I.O.; Okoro, C.J.; Taiwo, A.S.; Onuh, L.N.; Agbeboh, N.I.; Balogun, O.P.; Olubambi, P.A.; Lephuthing, S.S. Modern Trends in Recycling Waste Thermoplastics and Their Prospective Applications: A Review. *J. Compos. Sci.* **2023**, *7*, 198. [CrossRef]
30. Licea Saucedo, D.C.; Nuñez, R.G.; Vázquez Lepe, M.O.; Rodrigue, D. *Polymer Processing Technology to Recycle Polymer Blends BT—Recycled Polymer Blends and Composites: Processing, Properties, and Applications*; Springer International Publishing: Cham, Switzerland, 2023; pp. 111–132; ISBN 978-3-031-37046-5.
31. Huang, K.; Isayev, A. Comparison between Decrosslinking of Crosslinked High and Low Density Polyethylenes via Ultrasonically Aided Extrusion. *Polymer (Guildf)* **2015**, *70*, 290–306. [CrossRef]
32. Huang, K.; Isayev, A.I. Ultrasonic Decrosslinking of Crosslinked High-Density Polyethylene: Effect of Degree of Crosslinking. *RSC Adv.* **2014**, *4*, 38877–38892. [CrossRef]
33. Baek, B.K.; Shin, J.W.; Jung, J.Y.; Hong, S.M.; Nam, G.J.; Han, H.; Koo, C.M. Continuous Supercritical Decrosslinking Extrusion Process for Recycling of Crosslinked Polyethylene Waste. *J. Appl. Polym. Sci.* **2015**, *132*, 41442. [CrossRef]
34. Baek, B.K.; La, Y.H.; Lee, A.S.; Han, H.; Kim, S.H.; Hong, S.M.; Koo, C.M. Decrosslinking Reaction Kinetics of Silane-Crosslinked Polyethylene in Sub- and Supercritical Fluids. *Polym. Degrad. Stabil.* **2016**, *130*, 103–108. [CrossRef]
35. Wu, H.; Liang, M.; Lu, C. Morphological and Structural Development of Recycled Crosslinked Polyethylene During Solid-State Mechanochemical Milling. *J. Appl. Polym. Sci.* **2011**, *122*, 257–264. [CrossRef]
36. Zack, S.J.; Herrold, N.T.; Wakabayashi, K. Mechanochemical Modification of Crosslinked Low-Density Polyethylene: Effect of Solid-State Shear Pulverization on Crosslinks, Branches, and Chain Lengths. *SPE Polym.* **2022**, *3*, 152–162. [CrossRef]
37. Wu, H.; Liang, M.; Lu, C. Non-Isothermal Crystallization Kinetics of Peroxide-Crosslinked Polyethylene: Effect of Solid State Mechanochemical Milling. *Thermochim. Acta* **2012**, *545*, 148–156. [CrossRef]

38. Huang, K.; Isayev, A. Ultrasonic Decrosslinking of Peroxide Crosslinked HDPE in Twin Screw Extrusion: Part II Simulation and Experiment. *Polym. Eng. Sci.* **2016**, *57*, 1047–1061. [CrossRef]
39. Fang, J.; Zhang, L.; Sutton, D.; Wang, X.; Lin, T. Needleless Melt-Electrospinning of Polypropylene Nanofibres. *J. Nanomater.* **2012**, *2012*, 382639. [CrossRef]
40. Huang, K.; Isayev, A.; Zhong, J. Ultrasonic Decrosslinking of Crosslinked High-Density Polyethylene: Effect of Screw Design. *J. Appl. Polym. Sci.* **2014**, *131*, 40680. [CrossRef]
41. Isayev, A.; Huang, K. Decrosslinking of Crosslinked High-Density Polyethylene via Ultrasonically Aided Single-Screw Extrusion. *Polym. Eng. Sci.* **2014**, *54*, 2715–2730. [CrossRef]
42. *ASTM D2765*; Determination of Gel Content and Swell Ratio of Crosslinked Ethylene Plastics. ASTM Standard: West Conshohocken, PA, USA, 2016; pp. 1–8.
43. *ASTM D6814*; Standard Test Method for Determination of Percent Devulcanization of Crumb Rubber Based on Crosslink Density. ASTM Standard: West Conshohocken, PA, USA, 2002; pp. 1–5. [CrossRef]
44. Flory, P.J.; Rehner, J., Jr. Statistical Mechanics of Cross-Linked Polymer Networks II. Swelling. *J. Chem. Phys.* **1943**, *11*, 521–526. [CrossRef]
45. Gee, D.; Melia, T. Thermal Properties of Melt and Solution Crystallized Isotactic Polypropylene. *Die Makromol. Chem.* **2003**, *132*, 195–201. [CrossRef]
46. *ASTM E1225-20*; Standard Test Method for Thermal Conductivity of Solids Using the Guarded-Comparative-Longitudinal Heat Flow Technique. ASTM Standard: West Conshohocken, PA, USA, 2020; pp. 3–5. [CrossRef]
47. *ASTM D638-22*; Standard Test Method for Tensile Properties of Plastics. Nanomaterials. ASTM Standard: West Conshohocken, PA, USA, 2022; pp. 1–7.
48. *ASTM D2240-15*; Standard Test Method for Rubber Property—Durometer Hardness. ASTM Standard: West Conshohocken, PA, USA, 2015. [CrossRef]